Open access • Journal Article • DOI:10.1002/ADMI.201801664

Enzymes Immobilized on Carbon Nitride (C3N4) Cooperating with Metal Nanoparticles for Cascade Catalysis — Source link

Yangxin Wang, Ningning Zhang, René Hübner, Deming Tan ...+6 more authors

Institutions: Dresden University of Technology, Helmholtz-Zentrum Dresden-Rossendorf, Northwestern Polytechnical University, University of Southern Denmark

Published on: 01 Mar 2019 - Advanced Materials Interfaces (John Wiley & Sons Ltd)

Topics: Carbon nitride and Catalysis

Enzymes Immobilized on Carbon Nitride (C3N4) Cooperating with Metal Nanoparticles for Cascade Catalysis

Wang, Yangxin; Zhang, Ningning; Hübner, René; Tan, Deming; Löffler, Markus; Facsko, Stefan; Zhang, En; Ge, Yan; Qi, Zhenhui; Wu, Changzhu

Published in:
Advanced Materials Interfaces

DOI:
10.1002/admi.201801664

Publication date:
2019

Document version:
Accepted manuscript

DOI: 10.1002/ ((please add manuscript number))

Article type: Full Paper

Enzymes immobilized on carbon nitride (C_3N_4) cooperating with metal nanoparticles for cascade catalysis

Yangxin Wang, Ningning Zhang, René Hübner, Deming Tan, Markus Löffler, Stefan Facsko, En Zhang, Yan Ge, Zhenhui Qi* and Changzhu Wu**

Dr. Y. Wang, Prof. Y. Ge, Prof. Z. Qi

Sino-German Joint Research Lab for Space Biomaterials and Translational Technology, School of Life Sciences, Northwestern Polytechnical University

127 Youyi Xilu, Xi'an, Shaanxi, 710072, P. R. China
E-mail: ge@nwpu.edu.cn; qi@nwpu.edu.cn

Dr. Y. Wang, N. Zhang
Institute of Microbiology, Technische Universität Dresden

Zellescher Weg 20b, Dresden, 01217, Germany

Dr. R. Hübner, Dr. S. Facsko

Institute of Ion Beam Physics and Materials Research, Helmholtz-Zentrum Dresden-Rossendorf e.V. (HZDR)

Bautzner Landstraße 400, Dresden, 01328, Germany

D. Tan, E. Zhang

Department of Chemistry, Technische Universität Dresden

Bergstraße 66, Dresden, 01062, Germany

Dr. M. Löffler

Dresden Center for Nanoanalysis (DCN), Center for Advancing Electronics Dresden (cfaed), Technische Universität Dresden

Helmholtzstraße 18, Dresden, 01069, Germany

Prof. C. Wu

Danish Institute for Advanced Study (DIAS) and Department of Physics, Chemistry and Pharmacy, University of Southern Denmark

Campusvej 55, Odense, 5230, Denmark.

Email:wu@sdu.dk

Keywords: biohybrid catalyst, Pd nanoparticles, CalB, cascade reaction, carbon nitride

The exploration of effective platforms for immobilizing chemo- and biocatalysts to develop biohybrid catalysts is an attractive subject of practical interest. In this work, carbon nitride (C_3N_4) is used for the first time as a platform for the immobilization of metal catalyst (Pd nanoparticles) and biocatalyst (*Candida antarctica* lipase B, CalB) in a facile manner to prepare biohybrid catalyst. The optimal biohybrid catalyst inherits the intrinsic performance of both Pd nanoparticles and CalB, and shows high activity in the one-pot cascade reaction converting benzaldehyde to benzyl hexanoate at room temperature. With this proof-of-concept, it is expected that C_3N_4 can be utilized for immobilizing more types of chemo- and biocatalysts for perspective applications.

1. Introduction

Multistep cascade reactions catalysed by enzymes exist commonly in nature, and are of great importance for metabolic systems in organisms. Mimicking the natural systems, cascade reactions catalysed by chemo- and/or biocatalysts for organic synthesis have been intensively investigated in the past few decades.[1] Cascade reactions offer the possibility of combining different types of reactions in one pot, which can be used to develop new synthetic routes for specific compounds.[2]

Meanwhile, Cascade reactions can circumvent tedious workup of intermediates, avoiding the decomposition of unstable intermediates and saving time and cost.[3] Furthermore, due to the consumption of intermediates in cascade reactions, the reaction equilibrium is shifted, usually resulting in a higher conversion of substrates. Today, immobilizing chemo- and biocatalysts on solid materials to fabricate heterogeneous biohybrid catalysts for cascade reactions has attracted growing interests because of the easy products separation and simplified catalysts reuse. On the other hand, because of the co-immobilization of different catalysts on the same support, diffusion limitation of intermediates between active sites is reduced, which promotes the overall reaction efficiency in the one-pot process. To date, mesoporous silica[4], metal-organic frameworks (MOFs),[5] reduced graphene oxide[6], and polymeric matrices[7] have been utilized as supports for preparing biohybrid catalysts. It was found that intrinsic properties of these supports have a significant impact on the stability and distribution of immobilized chemocatalysts, while the compatibility between carriers and enzymes still remains a concern since enzymes are vulnerable in *in vitro* environment. Therefore, the judicial selection of solid supports is vitally important, and the task of seeking for new solid supports for developing biohybrid catalysts featuring new functions continues.

In the past decade, carbon nitride (C_3N_4) has emerged as a promising material for its outstanding performances in photocatalysis[8] and electrochemistry.[9] Besides, it has been also utilized for bioimaging and biomedical applications, where its good biocompatibility was verified through various methods, implying its great potential in the field of biocatalysis.[10] C_3N_4 was proven to coexist compatibly and work cooperatively with enzymes as a photocatalyst to regenerate nicotinamide adenine dinucleotide (NADH) in aqueous solution.[11] However, the application of C_3N_4 for stabilizing enzymes used in organic synthesis has not been reported yet, not to mention acting as solid support for preparing biohybrid catalysts for cascade reactions.

Within this context, we are encouraged to employ C_3N_4 as solid support to prepare biohybrid catalysts through immobilizing metal nanoparticles (NPs) and enzymes, which may show versatile and new functions in various fields due to the unique properties of C_3N_4. Metal NPs have been employed in fabricating biohybrid catalysts cooperatively with enzymes.[4a, 12] Due to the two-dimensional (2D) conjugated planes packed together with tris-*s*-triazine repeating units facilitating the binding of exotic atoms into its matrix, C_3N_4 can serve as superior scaffold for stabilizing metal atoms and/or NPs, such as Pd,[13] Pt,[14] Ag,[15] Au,[16] Cu,[17] and alloys.[18] Because of the large amount of N atoms, exceptional activity can be achieved due to the high ratio of low-coordinated metal atoms in these composite materials. Meanwhile, the dosage of noble metals can be minimized.[14a, 19] As is known, Pd NPs can catalyse a wide range of organic reactions, including reduction, oxidation, racemization, and coupling reactions,[20] while *Candida antarctica* lipase B (CalB) is an easily available lipase, which shows high activity and selectivity in catalysing esterification, hydrolysis and transesterification reactions under mild conditions.[21] In this work, Pd NPs and CalB were chosen for the concept-of-proof because they have been applied cooperatively for dynamic kinetic resolutions and cascade asymmetric synthesis in previous reports.[12a, 22] It is the first time that carbon nitride (C_3N_4) was used as support for the immobilization of metal catalyst (Pd NPs) and biocatalyst (CalB) in a facile manner to prepare biohybrid catalysts. The appropriate amount of immobilized Pd and CalB was carefully optimized, and the biohybrid catalysts were applied in a one-pot cascade reaction to produce benzyl hexanoate.

2. Results and Discussion

C_3N_4 was prepared *via* thermal decomposition of dicyandiamide in air at 550 °C for 4 h. The product was obtained as yellow powder and ground before use. In order to verify that C_3N_4 is able to

immobilize enzymes, CalB was initially immobilized on C_3N_4 through crosslinking using glutardialdehyde as crosslinker, which is a widely used method for enzyme immobilization.[23] The resulting product was denoted as CalB2@CN, in which the weight percentage of CalB was 2% to C_3N_4 theoretically. Based on thermal gravimetric analysis (TGA) results, typical C_3N_4 is stable up to 550 °C in air flow. In contrast, an obvious weight loss of 2.05% is observed at 250 °C in the TGA curve of CalB2@CN, which is caused by the decomposition of immobilized CalB (Figure S2a). The weight loss of 2.05% also indicates that the amount of immobilized CalB is close to the theoretical value of 2%. To test the activity of CalB after immobilization on C_3N_4, transesterification reaction between benzyl alcohol and ethyl hexanoate was conducted using CalB2@CN as catalyst at room temperature in toluene (**Figure 1**). Free CalB was also used to catalyse this reaction under identical conditions as a control experiment. To our delight, the activity of CalB was markedly improved after immobilization. When the reaction time was 6 h, the yield of benzyl hexanoate produced by CalB2@CN was 40.1%, while only a yield of 7.1% was obtained with free CalB (Figure 1b). The specific activity of CalB2@CN is 0.549 U mg^{-1}, which is 8 times higher than that of free CalB (0.066 U mg^{-1}) (Figure 1c). This result suggests that the physical and chemical interfaces of C_3N_4 may have some effects on the orientation and conformation of immobilized CalB, contributing to the enhanced activity.[24] Besides, free CalB easily aggregates in organic solvent, but the amphiphilic nature of C_3N_4 leads to an easy dispersion of CalB2@CN in toluene, which facilitates the contact between substrates and immobilized CalB and elevates its catalytic efficiency.[25]

In order to fabricate biohybrid catalysts for cascade reactions and avoid possible denaturation of CalB during the Pd immobilization process, Pd NPs were immobilized on C_3N_4 through impregnation-reduction method prior to the immobilization of CalB (**Scheme 1**). The resulting biohybrid catalysts were denoted as Pd0.5-CalB2@CN and Pd0.5-CalB10@CN. The number "0.5" means the theoretical weight percentage of Pd

to C_3N_4 is 0.5%, while the number "2" and "10" mean that the weight percentage of CalB to C_3N_4 is 2% and 10% in Pd0.5-CalB2@CN and Pd0.5-CalB10@CN, respectively. Based on inductively coupled plasma atomic emission spectroscopy (ICP-AES) analysis, the Pd content in Pd0.5@CN is determined as 0.48%, which is very close to the theoretical value. TGA results show that Pd0.5@CN can be stable up to about 520 °C, while an obvious weight loss of about 2.14% and 8.58% at 250 °C is observed from TGA curves of Pd0.5-CalB2@CN and Pd0.5-CalB10@CN, respectively. The weight loss beginning from 250 °C is derived from the decomposition of immobilized CalB, suggesting that the weight percentage of CalB in Pd0.5-CalB2@CN and Pd0.5-CalB10@CN is 2.14% and 8.58%, respectively, basically agreeing with the theoretical values (**Figure 2a**). The slight variations may be derived from the experimental deviations or incomplete immobilization of CalB.

The chemical composition of obtained biohybrid materials was investigated by powder X-ray diffraction (PXRD) and Fourier-transform infrared spectrometry (FTIR). In Figure 2b, the PXRD patterns of C_3N_4 and its derived hybrid materials are almost identical with each other. The disappearance of the Bragg reflections from the precursor dicyandiamide confirms its total conversion to C_3N_4. The characteristic peaks at 27.7° with an interlayer spacing of 3.3 Å correspond to the graphitic (002) plane of C_3N_4.[13b] The minor peaks at 13.2° are ascribed to the (100) planes in-planar tris-*s*-triazine structural packing motifs.[26] Noteworthily, no characteristic peaks derived from Pd NPs were observed in Pd0.5@CN, Pd0.5-CalB2@CN, and Pd0.5-CalB10@CN, which should be attributed to the low amount of Pd NPs and their small particle sizes. In the FTIR spectrum of C_3N_4, characteristic absorption bands of C=N

(1640 cm^{-1}), C-N (1246, 1327, and 1410 cm^{-1}), N-H (3205 cm^{-1}), and triazine vibration or breathing modes (806 cm^{-1}) are clearly demonstrated (Figure 2c).[26a] There is no obvious change in the spectra for the materials after immobilizing Pd NPs or CalB, suggesting the intact structure of C_3N_4. The textural properties of Pd0.5@CN, Pd0.5-CalB2@CN, and Pd0.5-CalB10@CN were obtained through nitrogen adsorption/desorption isotherms (Figure 2d). The total adsorption amount of N_2 for Pd0.5@CN decreased after the immobilization of CalB from 163 cm^3 g^{-1} to 128 (Pd0.5-CalB2@CN) and 113 cm^3 g^{-1} (Pd0.5-CalB10@CN), respectively, probably due to partial blocking of pores in C_3N_4 by immobilized CalB. A similar tendency was also observed in the changes of Brunauer-Emmett-Teller (BET) surface areas and total pore volumes (Table S1). Based on pore size distribution curves, only mesopores exist in Pd0.5@CN, Pd0.5-CalB2@CN, and Pd0.5-CalB10@CN, which are favorable to the mass transfer of substrates in catalytic reactions (Figure S5).

The morphologies of C_3N_4 and the hybrid catalysts were examined using scanning electron microscopy (SEM). Pristine C_3N_4 and Pd0.5@CN present layered porous structures, which is in accordance with previous reports (**Figure 3a** and S6a).[27] Meanwhile, a smooth layer on the top of Pd0.5-CalB2@CN and Pd0.5-CalB10@CN can be clearly observed, which is believed to be the immobilized CalB layer (Figure 3b and S6b). These observations indicate the successful immobilization of CalB on the surface of C_3N_4. Transmission electron microscopy (TEM) characterization was performed to investigate the morphology and distribution of Pd NPs in Pd0.5-CalB2@CN (Figure 3c). The average diameter of Pd NPs in Pd0.5-CalB2@CN is 3.0±0.6 nm, which is smaller compared to that in previous reports due to the low

loading amount of Pd.[10d, 28] High-angle annular dark-field scanning transmission electron microscopy (HAADF-STEM) of Pd0.5-CalB2@CN combined with element mapping based on energy-dispersive X-ray spectroscopy (EDXS) clearly confirm the existence of Pd NPs and show their distribution all over the biohybrid catalyst (Figure 3d).

X-ray photoelectron spectroscopy (XPS) was used to survey the chemical environment around C, N, and Pd atoms in the solid samples. In the survey spectra, signals from C and N elements can be observed in all samples (**Figure 4a**). The signals from O element are weak in C_3N_4 and Pd0.5@CN, which was probably derived from the adsorbed O species. However, the signals from O elements increased significantly in Pd0.5-CalB2@CN and Pd0.5-CalB10@CN after immobilizing CalB, which contains a large number of O atoms. Due to the low amount of Pd in Pd0.5@CN, Pd0.5-CalB2@CN, and Pd0.5-CalB10@CN, signals of Pd in XPS survey spectra are almost invisible. XPS core level spectra of C 1s are displayed in Figure 4b. One prominent peak with a binding energy of 288.1 eV is observed in C 1s spectrum of pristine C_3N_4, corresponding to N-C=N coordination. No obvious change in C 1s spectrum is observed after immobilizing Pd NPs except for the slight strengthening of the peak at 284.8 eV, which is ascribed to surface adventitious carbon.[13c] However, C 1s spectra of Pd0.5-CalB2@CN and Pd0.5-CalB10@CN can be resolved into three peaks. The newly appeared peak at 285.8 eV and significantly strengthened peak at 284.8 eV are ascribed to C-N/C-O and C-C species in CalB, respectively. The N 1s spectrum of C_3N_4 can be resolved into three peaks at 397.8, 398.5, and 399.9 eV, corresponding to the C-N=C, N-$(C)_3$, and C-N-H moieties, respectively (Figure 4c).[27]

After loading Pd NPs, the peaks shifted positively to 297.9, 398.8, and 400.1 eV, respectively, indicating a strong interaction between Pd atoms and N atoms.[29] The signals from Pd species can be clearly observed in core level spectra. As illustrated in Figure 4d, the peaks at 335.2 and 340.3 eV can be attributed to Pd(0) $3d_{3/2}$ and Pd(0) $3d_{5/2}$, while peaks at 337.1 and 342.2 eV are ascribed to Pd(II) $3d_{3/2}$ and Pd(II) $3d_{5/2}$, respectively, showing the co-existence of Pd(0) and Pd(II) species.[30] The contribution of Pd(0) and Pd(II) species to the total Pd can be estimated from the corresponding peak areas. It was found that the proportion of Pd(0) and Pd(II) was 40.4% and 59.6% in Pd0.5@CN, respectively. The high proportion of Pd(II) species is probably due to the highly dispersed tiny Pd(0) clusters within C_3N_4 support, which has a large contact surface area with air and is easy to be re-oxidized into Pd(II) species. The proportion of Pd(II) species decreased to 55.0% and 22.0% in Pd0.5-CalB2@CN and Pd0.5-CalB10@CN, respectively. The decrement of Pd(II) species is probably because the immobilized CalB covers the surface of Pd clusters partially, which inhibits the contact of Pd clusters with O_2 in air.

A two-step one-pot cascade reaction transferring benzaldehyde into benzyl hexanoate was chosen as a model reaction to evaluate the catalytic performance of the biohybrid catalyst. Benzaldehyde was first reduced into benzyl alcohol using molecular H_2 catalysed by Pd, which then further reacted with ethyl hexanoate into benzyl hexanoate propelled by CalB. The plausible reaction pathway was given in Figure S7.[31] Initially, the reaction was performed in toluene (250 μL) containing benzaldehyde (400 mM) and ethyl hexanoate (800 mM) in the presence of Pd0.5-CalB2@CN with a H_2 balloon. After 2 h, the conversion of benzaldehyde was 27.6%,

and the yield of final product benzyl hexanoate was 11.1% (Figure S8). In control experiments, when Pd0.5@CN was used as catalyst, benzaldehyde was totally converted into benzyl alcohol. No reaction took place when CalB2@CN was used, confirming that the cascade reaction was catalysed cooperatively by Pd NPs and CalB.

To have a clear insight into the influence of Pd content in the catalytic efficiency, besides Pd0.5@CN, two additional materials Pd0.1@CN and Pd2.5@CN were prepared (seeing details in experimental section). The distribution of Pd NPs in these materials was observed using TEM (Figure S9). Besides, mesoporous SiO_2 was also employed as support for Pd NPs, obtaining a control sample Pd0.5@SiO_2, in which the Pd content is 0.48% based on ICP-AES characterization. Their catalytic activity was first evaluated through hydrogenation reaction of benzaldehyde. It has been reported that Pd NPs immobilized in C_3N_4 show remarkable catalytic activity in reduction reactions.[13c] The reduction of aldehydes with hydrogen catalysed by Pd can be performed in a mild manner. The reactions were performed in the presence of benzaldehyde (0.1 mmol) and solid catalyst (20 mg) in H_2O (250 μL) with a H_2 balloon for 1 h under room temperature. As shown in **Figure 5a**, Pd2.5@CN containing the most amount of Pd exhibits the highest activity since the yield was found to be 96.2%. Though Pd0.5@CN and Pd0.5@SiO_2 contain the same amount of Pd, the yield of benzyl alcohol catalysed by Pd0.5@CN is 80.0%, which is almost 2.8 times comparing with Pd0.5@SiO_2, indicating that C_3N_4 is indeed an attractive support for the metal catalyst. Pd0.1@CN only gave a poor yield of 4.2% due to the low amount of Pd. When considering the catalytic efficiency of Pd in these catalysts, turnover frequency (TOF) was calculated, which is defined as the number of moles of

benzaldehyde converted over per mole of Pd per unit time (h) (Figure 5b). It was found that Pd0.5@CN displays the highest TOF of 85.1 h^{-1}, while Pd0.1@CN and Pd2.5@CN only gave a TOF of 22.3 and 20.5 h^{-1}, respectively, indicating that the Pd NPs in Pd0.5@CN have a higher efficiency than those in Pd0.1@CN and Pd2.5@CN. TOF of Pd0.5@SiO_2 was also much lower than that of Pd0.5@CN, confirming the superiority of C_3N_4 comparing with SiO_2 as support for Pd NPs.

As our aim is to establish biohybrid catalysts for cascade reactions, Pd0.1@CN, Pd2.5@CN, and Pd0.5@SiO_2 were further utilized to immobilize CalB, and hybrid catalysts Pd0.1-CalB2@CN, Pd2.5-CalB2@CN, and Pd0.5-CalB2@SiO_2 were obtained, respectively. These catalysts contain almost the same amount of CalB but different amount of Pd. Their catalytic performances were also evaluated through the cascade reaction converting benzaldehyde to benzyl hexanoate. It was found that after immobilizing CalB, the catalytic efficiency of Pd0.5-CalB2@CN is the highest among all the tested materials when normalizing the amount of produced benzyl hexanoate (mol) per h in the initial 2 h by the amount of Pd (mol) (**Figure 6a**), even though the overall yield of Pd2.5-CalB@CN is the highest due to its largest amount of immobilized Pd (Figure S10). Considering the source scarce and high expense of Pd, we chose 0.5% as the optimized loading amount of Pd. Influence of the amount of CalB was also investigated. As shown in Figure 6b, when the amount of CalB increases from 0.5% to 2%, the yield of benzyl hexanoate increases from 47.4% to 78.9%. However, when the amount of CalB was further increased to 10%, the yield of benzyl hexanoate rapidly dropped to only 32.2%. The decreased yield along with the increment of CalB can be attributed to the large amount of CalB covering the surface

of C_3N_4 containing Pd, inhibiting the contact between substrates and Pd NPs. After these optimizations, the optimal biohybrid catalyst with suitable Pd and CalB loading was established, which turns out to be 0.5% and 2%, respectively.

In biocatalysis, the substrate concentration usually has a significant impact on catalytic behavior. As shown in Figure S11, when the concentration of benzaldehyde decreased from 400 mM to 200 mM, and the concentration of ethyl hexanoate decreased from 800 mM to 400 mM, equilibrium of the reaction was reached in a shorter time. The yield of benzyl hexanoate achieved 81.7% at 12 h and kept steady with prolonging reaction time when the reaction concentration was halved (Figure S11a). During the reaction, the yield of benzyl alcohol increased sharply to reach a peak value in the initial 2 h or 4 h when the initial concentration of benzaldhyde was 200 mM or 400 mM, respectively, indicating that the second-step transesterification reaction is the rate-limiting step in this cascade reaction (Figure S11b). Benzaldehyde was totally converted within 2 or 4 h when the initial concentration was 200 or 400 mM, respectively (Figure S11c). The reusability of the biohybrid catalyst Pd0.5-CalB2@CN was also investigated. As shown in Figure S12, after used for 4 times, yield of the final product was only 25.7%, while the yield of benzyl alcohol remained as high as 58.8%, indicating that the activity of CalB in biohybrid catalyst degrades more seriously than that of Pd. The reused Pd0.5-CalB2@CN was also analysed with SEM and TEM. In SEM image, the shape of C_3N_4 was well conserved but the smooth CalB layer disappeared (Figure S13). TEM and element mapping images show no obvious change of Pd NPs after reuse (Figure S14). A leaching test after the first-run reaction revealed that neither Pd nor CalB was detected in reaction media. All the

experiments suggest that the deactivation of the enzyme CalB should be mainly accounted for the decreased yield of benzyl hexanoate.

3. Conclusion

In summary, we described for the first time the application of C_3N_4 as support for the construction of biohybrid catalyst through stepwise immobilizing Pd NPs and CalB. Due to the unique structure of C_3N_4 with an abundant amount of N atoms, the immobilized Pd NPs show very high catalytic efficiency in the hydrogenation of benzaldehyde using H_2 under room temperature. CalB was immobilized on the surface of C_3N_4 facilely using glutardialdehyde as crosslinker, and it was found that the immobilized CalB on C_3N_4 show remarkably superior activity than free CalB. After careful optimization, the biohybrid catalyst containing 0.5% Pd and 2% CalB showed the best catalytic efficiency in catalysing a one-pot cascade reaction transferring benzaldehyde to benzyl hexanoate. This work demonstrates the possibility that C_3N_4 can be used as a new type of platform where chemo- and biocatalysts can be immobilized and used for constructing biohybrid catalysts for cascade reactions. Since C_3N_4 has been proven to be a versatile material in various fields, it could be envisioned that C_3N_4-based biohybrid catalysts might be employed in more advanced applications with fascinating perspectives in future.

4. Experimental Section

General Information: Unless otherwise noted, all materials, reagents, and solvents were obtained from commercial suppliers and used without further purification. *Candida antarctica* lipase B (CalB) was purchased from c-LEcta GmbH (Leipzig, Germany), and the weight percentage of pure CalB is

about 10% based on Bradford test (**Fig. S1**).[32] Mesoporous SiO_2 was prepared following the reported method.[33] Bradford test was performed on TECAN infinite M200. Thermogravimetric analysis (TGA) was carried out with a TG 50 modular unit and a TC 15 TA controller (Mettler-Toledo, Giessen, Germany) by heating samples from 25 ^{o}C to 800 ^{o}C in a dynamic air atmosphere with a heating rate of 10 ^{o}C min^{-1}. Fourier transform infrared spectroscopy (FTIR) spectra were recorded on a FTIR spectrometer Tensor II (Bruker) with an ATR unit. Powder X-ray diffraction (PXRD) was performed on a PANalytical X'Pert Pro Powder diffractometer with Debye-Scherrer geometry equipped with a Ge(111)-monochromator, a rotating sample stage, and a PIXcel detecotor, using Cu $K\alpha_1$ radiation (λ = 154.06 pm). The data were collected in reflection mode using a divergence slit that kept the illuminated sample area constant. Scanning electron microscope (SEM) images were recorded with a Gemini 500 (Carl Zeiss, Germany) system. Bright-field TEM images were recorded on a Titan 80-300 (FEI) microscope operated at an accelerating voltage of 300 kV. High-angle annular dark-field scanning transmission electron microscopy (HAADF-STEM) imaging and spectrum imaging based on energy-dispersive X-ray spectroscopy (EDXS) were performed at 200 kV with a Talos F200X microscope equipped with an X-FEG electron source and a Super-X EDXS detector system (FEI). Prior to TEM analysis, the specimen mounted in a high-visibility low-background holder was placed for 2 s into a Model 1020 Plasma Cleaner (Fischione) to remove contamination. TEM specimens were prepared by dropping the solution under investigation with several microliters of sample well-dispersed in distilled water onto a carbon-coated copper grid (400 mesh, S160-4, Plano GmbH) and drying it under ambient conditions. X-ray photoelectron spectroscopy (XPS) spectra were taken with a Microlab 310 system by Thermo Fisher Scientific using the Mg K-alpha line of a dual-anode X-ray source. ^{1}H and ^{13}C NMR spectra were recorded by using a Bruker AVANCE III NMR spectrometer at 400 and 100 MHz, respectively, with tetramethylsilane (TMS) as an internal standard. Inductively coupled plasma-optical emission spectroscopy (ICP-OES) measurements were carried out on a

Perkin-Elmer Optima 7000DV optical emission spectrometer. Gas chromatography (GC) analysis was performed on a Shimadzu GC2010 PLUS gas chromatograph equipped with a BPX5 column (25 m × 0.22 mm) using a flame ionization detector (FID). Yield in catalytic reactions was calculated referring to the theoretically possible total mole of product.

Preparation of C_3N_4 (CN): C_3N_4 was synthesized by heating dicyandiamide (10 g) from room temperature to 550 ^oC at a heating rate of 3 $^oC\ min^{-1}$ in a covered alumina crucible placed inside a muffle furnace. After calcination at 550 ^oC for 4 h, the prepared C_3N_4 (5 g) was naturally cooled to room temperature and obtained as a pale yellow powder.

Preparation of CalB2@CN: Carbon nitride (800 mg) was dispersed in isopropanol (120 mL) with ultrasonication for 5 min. With stirring, solution of CalB (160 mg) in 40 mL phosphate buffer (100 mM, pH = 7) was added to the suspension. The stirring was continued for 5 min, then a glutardialdehyde solution (12 mL, 25 wt% in water) was added, and the reaction was kept stirred under room temperature for 20 h. Finally the solid was isolated with centrifugation (8000 rpm) and washed with water (4 × 40 mL) before lyophilized. The obtained pale yellow powder was denoted as CalB2@CN, and the number "2" means that the theoretical weight percentage of CalB to C_3N_4 is 2%.

Preparation of Pd0.5@CN, Pd0.1@CN, and Pd2.5@CN: C_3N_4 (1.00 g) was dispersed in deionized water (100 mL) with ultrasonication for 15 min. An aqueous solution of Na_2PdCl_4 (10 mM, 4.72 mL) was added, and the resulted suspension was stirred at room temperature for 1 h. Subsequently, a freshly prepared aqueous solution of $NaBH_4$ (500 mM, 1.4 mL) was added into this mixture. After stirred for another 1 h, the solid was filtered and washed with deionized water (3 × 40 mL) and ethanol (3 × 40 mL). Finally, the product Pd0.5@CN was dried in an oven at 50 ^oC overnight. The numbers 0.5 means that the weight percentage of Pd to C_3N_4 is 0.5%. The exact content of Pd in Pd0.5@CN is 0.48% based on ICP-AES analysis.

Pd0.1@CN was prepared following the same procedure except that aqueous solution of Na_2PdCl_4 (10 mM, 0.944 mL) and $NaBH_4$ (500 mM, 0.28 mL) was used. And Pd2.5@CN was also prepared following the same procedure except that aqueous solution of Na_2PdCl_4 (10 mM, 23.6 mL) and $NaBH_4$ (500 mM, 7 mL) was used. The numbers "0.1" and "2.5" mean that the weight percentage of Pd to C_3N_4 is 0.1% and 2.5%, respectively. The exact content of Pd in Pd0.1@CN and Pd2.5@CN is 0.08% and 2.41% based on ICP-AES analysis, respectively.

Preparation of Pd0.5-CalB2@CN: Pd0.5@CN (800 mg) was dispersed in isopropanol (120 mL) with ultrasonication for 5 min. With stirring, solution of CalB (160 mg) in 40 mL phosphate buffer (100 mM, pH = 7) was added to the suspension. The stirring was continued for 5 min, then a glutardialdehyde solution (12 mL, 25 wt% in water) was added and the reaction was kept stirred under room temperature for 20 h. Finally the solid was isolated through centrifugation (8000 rpm) and washed with water (4 ×

40 mL) before lyophilized. Theobtained grey powder was denoted as Pd0.5-CalB2@CN.

Pd0.1-CalB2@CN and Pd2.5-CalB2@CN were prepared following the same method except that Pd0.1@CN and Pd2.5@CN were used, respectively.

Preparation of Pd0.5-CalB0.5@CN: Pd0.5@CN (300 mg) was dispersed in isopropanol (45 mL) with ultrasonication for 5 min. With stirring, a solution of CalB (15 mg, raw material) in 15 mL phosphate buffer (100 mM, pH = 7) was added to the suspension. The stirring was continued for 5 min, then a glutardialdehyde solution (1.12 mL, 25 wt% in water) was added and the reaction was kept stirred under room temperature for 20 h. Finally the solid was isolated through centrifugation (8000 rpm) and washed with water (4 × 20 mL) before lyophilized. The resulting grey powder was denoted as Pd0.5-CalB0.5@CN.

Preparation of Pd0.5-CalB1@CN: Pd0.5@CN (300 mg) was dispersed in isopropanol (45 mL) with ultrasonication for 5 min. With stirring, solution of CalB (30 mg) in 15 mL phosphate buffer (100 mM, pH = 7) was added to the suspension. The stirring was continued for 5 min, then a glutardialdehyde solution (2.25 mL, 25 wt% in water) was added and the reaction was kept stirred under room temperature for 20 h. Finally the solid was isolated through centrifugation (8000 rpm) and washed with water (4 × 20 mL) before lyophilized. The resulted grey powder was denoted as Pd0.5-CalB1@CN.

Preparation of Pd-10CalB@CN: Pd@CN (800 mg) was dispersed in isopropanol (120 mL) with ultrasonication for 5 min. With stirring, solution of CalB (800 mg) in 200 mL phosphate buffer (100 mM, pH = 7) was added to the suspension. The stirring was continued for 5 min, then a glutardialdehyde solution (60 mL, 25 wt% in water) was added and the reaction was kept stirred under room temperature for 20 h. Finally the solid was isolated through centrifugation (8000 rpm) and washed with water (4 × 40 mL) before lyophilized. The resulted grey powder was denoted as Pd0.5-CalB10@CN.

Preparation of Pd0.5@SiO_2 and Pd0.5-CalB2@SiO_2: Silica particles (500 mg) was dispersed in deionized water (50 mL) with ultrasonication for 15 min. An aqueous solution of Na_2PdCl_4 (10 mM, 2.36 mL) was added, and the resulted suspension was stirred at room temperature for 1 h. Afterwards, a freshly prepared aqueous solution of $NaBH_4$ (500 mM, 0.7 mL) was added into this mixture. After stirred for another 1 h, the solid was filtered and washed with deionized water (3 × 40 mL) and ethanol (3 × 40 mL). Finally, the product Pd0.5@SiO_2 was dried in an oven at 50 ^oC overnight. The number "0.5" means that the theoretical weight percentage of immobilized Pd to SiO_2 is 0.5%. The exact Pd content in Pd@SiO_2 is 0.48% based on ICP-AES analysis.

Pd0.5@SiO_2 (200 mg) was dispersed in isopropanol (30 mL) with ultrasonication for 5 min. Under stirring, solution of CalB (40 mg) in 10 mL phosphate buffer (100 mM, pH = 7) was added to the suspension. The stirring was continued for 5 min, then a glutardialdehyde solution (12 mL, 25 wt% in water) was added and the reaction was kept stirred under room temperature for 20 h. Finally the solid was isolated through centrifugation (8000 rpm) and washed with water (4 × 10 mL) before lyophilized. The

obtained solid was denoted as Pd0.5-CalB2@SiO_2. The number "2" means that the weight percentage of immobilized CalB to SiO_2 is 2%.

Procedure for transesterification between benzyl alcohol and ethyl hexanoate: CalB2@CN (20 mg) or free CalB (4 mg) was added to 250 μL toluene solution containing benzyl alcohol (10.4 μL, 0.1 mmol) and ethyl hexanoate (33.2 μL, 0.2 mmol) in a vial. After tightly sealed, the vial was shaken under room temperature at a speed of 400 rpm. At time intervals, 5 μL reaction mixture was withdrawn, diluted to 100 μL and centrifuged at 14800 rpm for 30 s to remove the solid catalyst. Then the solution was analyzed with GC to determine the yield of benzyl hexanoate.

Typical procedure for hydrogenation of benzaldehyde: Benzaldehyde (10.2 μL, 0.1 mmol) was added to a dispersion of solid catalyst (20 mg) in water (250 μL) in a Schlenk tube. The tube was purged with H_2 for three times to remove air, and the reaction mixture was stirred with a balloon of H_2 at room temperature for a given time. The reaction mixture was extracted with ethyl acetate (3 × 500 μL). The combined organic layer was analyzed with GC to determine the yield of benzyl alcohol.

Typical procedure for cascade reactions: To a Schlenk tube with solid catalyst (20 mg), organic solvent solution (250 μL) containing benzaldehyde (10.2 μL, 0.1 mmol) and ethyl hexanoate (33.2 μL, 0.2 mmol) was added. The Schlenk tube was purged with H_2 for three times to remove air, and the reaction mixture was stirred with a

balloon of H_2 at room temperature for a given time. After the reaction was finished, the solid was removed through centrifugation (6000 rpm, 1 min), and organic solvent was analyzed by GC after diluted by 10 times.

Reuse of Pd0.5-2CalB@CN: Toluene solution (250 μL) containing benzaldehyde (5.1 μL, 0.05 mmol) and ethyl hexanoate (16.6 μL, 0.1 mmol) was added to a Schlenk tube with Pd-2CalB@CN (20 mg). The Schlenk tube was purged with H_2 for three times to remove air, and the reaction mixture was stirred with a balloon of H_2 at room temperature for 12 h. After the reaction was finished, the solid was isolated through centrifugation (6000 rpm, 1 min), and organic solvent was analyzed by GC after diluted by 10 times. The recovered solid was washed with toluene (3 × 1 mL), dried in air under room temperature, and used for the next run of catalytic reaction following the same procedure.

Supporting Information

Supporting Information is available from the Wiley Online Library or from the author.

Acknowledgements

We gratefully acknowledge financial support from the Thousand Talents Program of China (1800-16GH030121), China Postdoctoral Science Foundation (2017M623231), and Fundamental Research Funds for the Central Universities (3102018zy051). C. W. thanks DFG (WU 814/1-1) for financial support. The use of HZDR Ion Beam Center TEM facilities and the funding of TEM Talos by the German Federal Ministry of Education of Research (BMBF), Grant No. 03SF0451 in the framework of HEMCP are acknowledged. M. L. acknowledges support by Deutsche Forschungsgemeinschaft *via* the cluster of excellence EXC1056 “Center for Advancing Electronics Dresden” (cfaed). We thank Mr. Matthias Kluge for his assistance with TGA characterization, Mr. Mingchao Wang for his assistance with FTIR characterization, and Mr. Yujian Zhou for his assistance with ICP-AES characterization. We thank the Analytical & Testing Center of NPU for the characterization instruments. We thank Prof. Marion B. Ansorge-Schumacher (TU Dresden) for valuable discussions and support, and Prof. Rainer Jordan (TU Dresden) for providing lab facility.

Received: ((will be filled in by the editorial staff))
Revised: ((will be filled in by the editorial staff))
Published online: ((will be filled in by the editorial staff))

References

[1] a) H. Wang, Z. Zhao, Y. Liu, C. Shao, F. Bian, Y. Zhao, *Sci. Adv.* **2018**, *4*, eaat2816; b) L. Marx, N. Ríos-Lombardía, J. F. Farnberger, W. Kroutil, A. I. Benitez-Mateos, F. Lopez-Gallego, F. Morís, J. Gonzalez-Sabin, P. Berglund, *Adv. Synth. Catal.* **2018**, *360*, 2157-2165; c) C. A. Denard, H. Huang, M. J. Bartlett, L. Lu, Y. Tan, H. Zhao, J. F. Hartwig, *Angew. Chem. Int. Ed.* **2014**, *53*, 465-469; d) N. Scalacci, G. W. Black, G. Mattedi, N. L. Brown, N. J. Turner, D. Castagnolo, *ACS Catal.* **2017**, *7*, 1295-1300; e) E. Liardo, N. Ríos-Lombardía, F. Morís, F. Rebolledo, J. González-Sabín, *ACS Catal.* **2017**, *7*, 4768-4774; f) H. Zhang, X. Liang, L. Han, F. Li, *Small* **2018**, 1803256; g) L. Xin, C. Zhou, Z. Yang, D. Liu, *Small* **2013**, *9*, 3088-3091; h) S. F. van Dongen, M. Nallani, J. J. Cornelissen, R. J. Nolte, J. C. van Hest, *Chem. Eur. J.* **2009**, *15*, 1107-1114.

[2] a) A. Sib, T. A. M. Gulder, *Angew. Chem. Int. Ed.* **2018**, DOI: 10.1002/anie.201802176; b) T. Hayashi, D. Hilvert, A. P. Green, *Chem. Eur. J.* **2018**, *24*, 11821-11830; c) S. Schmidt, H. C. Buchsenschutz, C. Scherkus, A. Liese, H. Groger, U. T. Bornscheuer, *ChemCatChem* **2015**, *7*, 3951-3955; d) E. Ricca, B. Brucher, J. H. Schrittwieser, *Adv. Synth. Catal.* **2011**, *353*, 2239-2262.

[3] a) F. Rudroff, M. D. Mihovilovic, H. Gröger, R. Snajdrova, H. Iding, U. T. Bornscheuer, *Nat. Catal.* **2018**, *1*, 12-22; b) Á. Gómez Baraibar, D. Reichert, C. Mügge, S. Seger, H. Gröger, R.

Kourist, *Angew. Chem. Int. Ed.* **2016**, *55*, 14823-14827; c) R. Ye, J. Zhao, B. B. Wickemeyer, F. D. Toste, G. A. Somorjai, *Nat. Catal.* **2018**, *1*, 318-325.

[4] a) K. Engstrom, E. V. Johnston, O. Verho, K. P. Gustafson, M. Shakeri, C. W. Tai, J. E. Bäckvall, *Angew. Chem. Int. Ed.* **2013**, *52*, 14006-14010; b) Y. C. Lee, S. Dutta, K. C. Wu, *ChemSusChem* **2014**, *7*, 3241-3246; c) M. Egi, K. Sugiyama, M. Saneto, R. Hanada, K. Kato, S. Akai, *Angew. Chem. Int. Ed.* **2013**, *52*, 3654-3658; d) N. Zhang, R. Hübner, Y. Wang, E. Zhang, Y. Zhou, S. Dong, C. Wu, *ACS Appl. Nano Mater.* **2018**, *1*, 6378-6386.

[5] a) S. Tadepalli, J. Yim, S. Cao, Z. Wang, R. R. Naik, S. Singamaneni, *Small* **2018**, *14*, 1702382; b) W. Chen, M. Vázquez-González, A. Zoabi, R. Abu-Reziq, I. Willner, *Nat. Catal.* **2018**, *1*, 689-695; c) X. Wu, J. Ge, C. Yang, M. Hou, Z. Liu, *Chem. Commun.* **2015**, *51*, 13408-13411; d) Y. Wang, N. Zhang, E. Zhang, Y. Han, Z. Qi, M. B. Ansorge-Schumacher, Y. Ge, C. Wu, *Chem. Eur. J.* 10.1002/chem.201805680.

[6] F. Zhao, H. Li, Y. Jiang, X. Wang, X. Mu, *Green Chem.* **2014**, *16*, 2558-2565.

[7] a) Q. Chen, H. Schonherr, G. J. Vancso, *Small* **2009**, *5*, 1436-1445; b) D. Wang, G. Zhang, Y. Zhang, L. Xin, Y. Dong, Y. Liu, D. Liu, *Small* **2017**, *13*, 1700594.

[8] a) S. Cao, J. Low, J. Yu, M. Jaroniec, *Adv. Mater.* **2015**, *27*, 2150-2176; b) Z. Chen, T. Fan, X. Yu, Q. Wu, Q. Zhu, L. Zhang, J. Li, W. Fang, X. Yi, *J. Mater. Chem. A* **2018**, *6*, 15310-15319; c) W. Yu, S. Zhang, J. Chen, P. Xia, M. H. Richter, L. Chen, W. Xu, J. Jin, S. Chen, T. Peng, *J. Mater. Chem. A* **2018**, *6*, 15668-15674; d) J. Zhu, P. Xiao, H. Li, S. A. C. Carabineiro, *ACS Appl. Mater. Interfaces* **2014**, *6*, 16449-16465; e) J. Fu, J. Yu, C. Jiang, B. Cheng, *Adv. Energy Mater.* **2018**, *8*, 1701503; f) J. Yin, Z. Li, Y. Cai, Q. Zhang, W. Chen, *Chem. Commun.* **2017**, *53*, 9430-9433; g) L. Sung, T. Du, C. Hu, J. Chen, J. Lu, Z. Lu, H. Han, *ACS Sustainable Chem. Eng.* **2017**,

5, 8693-8701; h) Y. Peng, B. Lu, L. Chen, N. Wang, J. E. Lu, Y. Ping, S. Chen, *J. Mater. Chem. A* **2017**, *5*, 18261-18269; i) H. Huang, K. Xiao, N. Tian, F. Dong, T. Zhang, X. Du, Y. Zhang, *J. Mater. Chem. A* **2017**, *5*, 17452-17463; j) Y. Hong, C. Li, D. Li, Z. Fang, B. Luo, X. Yan, H. Shen, B. Mao, W. Shi, *Nanoscale* **2017**, *9*, 14103-14110; k) Z. Ding, X. Chen, M. Antonietti, X. Wang, *ChemSusChem* **2011**, *4*, 274-281.

[9] a) F. K. Kessler, Y. Zheng, D. Schwarz, C. Merschjann, W. Schnick, X. Wang, M. J. Bojdys, *Nat. Rev. Mater.* **2017**, *2*, 17030; b) Y. Dong, Q. Wang, H. Wu, Y. Chen, C. Lu, Y. Chi, H. Yang, *Small* **2016**, *12*, 5376-5393; c) L. Chen, J. Song, *Adv. Funct. Mater.* **2017**, *27*, 1702695.

[10] a) S. E. Rodil, R. Olivares, H. Arzate, S. Muhl, *Diam. Relat. Mater.* **2003**, *12*, 931-937; b) D. Liu, J. Tu, R. Chen, C. Gu, *Surf. Coat. Technol.* **2011**, *206*, 165-171; c) X. Zhang, X. Xie, H. Wang, J. Zhang, B. Pan, Y. Xie, *J. Am. Chem. Soc.* **2013**, *135*, 18-21; d) M. Ayan-Varela, S. Villar-Rodil, J. I. Paredes, J. M. Munuera, A. Pagan, A. A. Lozano-Perez, J. L. Cenis, A. Martinez-Alonso, J. M. Tascon, *ACS Appl. Mater. Interfaces* **2015**, *7*, 24032-24045; e) Z. Zhang, R. Xu, Z. Wang, M. Dong, B. Cui, M. Chen, *ACS Appl. Mater. Interfaces* **2017**, *9*, 34736-34743; f) G. Q. Yang, T. J. Chen, B. Feng, J. Weng, K. Duan, J. X. Wang, X. B. Lu, *J. Alloy. Compd.* **2019**, *770*, 823-830.

[11] a) J. Liu, M. Antonietti, *Energy Environ. Sci.* **2013**, *6*, 1486-1493; b) J. W. Ko, W. S. Choi, J. Kim, S. K. Kuk, S. H. Lee, C. B. Park, *Biomacromolecules* **2017**, *18*, 3551-3556.

[12] a) T. Görbe, K. P. J. Gustafson, O. Verho, G. Kervefors, H. Zheng, X. Zou, E. V. Johnston, J.-E. Bäckvall, *ACS Catal.* **2017**, *7*, 1601-1605; b) J. M. Foulkes, K. J. Malone, V. S. Coker, N. J. Turner, J. R. Lloyd, *ACS Catal.* **2011**, *1*, 1589-1594.

[13] a) J. Sun, Y. Fu, G. He, X. Sun, X. Wang, *Appl. Catal. B-Environ.* **2015**, *165*, 661-667; b) T. Bhowmik, M. K. Kundu, S. Barman, *ACS Catal.* **2016**, *6*, 1929-1941; c) X. Xu, J. Luo, L. Li, D.

Zhang, Y. Wang, G. Li, *Green Chem.* **2018**, *20*, 2038-2046; d) G. Vile, D. Albani, M. Nachtegaal, Z. Chen, D. Dontsova, M. Antonietti, N. Lopez, J. Perez-Ramirez, *Angew. Chem. Int. Ed.* **2015**, *54*, 11265-11269; e) X. Huang, Y. Xia, Y. Cao, X. Zheng, H. Pan, J. Zhu, C. Ma, H. Wang, J. Li, R. You, S. Wei, W. Huang, J. Lu, *Nano Res.* **2017**, *10*, 1302-1312; f) J. Sun, Y. Fu, G. He, X. Sun, X. Wang, *Appl. Catal. B-Environ.* **2015**, *165*, 661-667.

[14] a) G. Gao, Y. Jiao, E. R. Waclawik, A. Du, *J. Am. Chem. Soc.* **2016**, *138*, 6292-6297; b) X. Li, W. Bi, L. Zhang, S. Tao, W. Chu, Q. Zhang, Y. Luo, C. Wu, Y. Xie, *Adv. Mater.* **2016**, *28*, 2427-2431; c) X. Chen, L. Zhang, B. Zhang, X. Guo, X. Mu, *Sci. Rep.* **2016**, *6*, 28558; d) H. Huang, S. Yang, R. Vajtai, X. Wang, P. M. Ajayan, *Adv. Mater.* **2014**, *26*, 5160-5165; e) K. Li, Z. Zeng, L. Yana, S. Luo, X. Luo, M. Huo, Y. Guo, *Appl. Catal. B-Environ.* **2015**, *165*, 428-437.

[15] a) W. Bing, Z. Chen, H. Sun, P. Shi, N. Gao, J. Ren, X. Qu, *Nano Res.* **2015**, *8*, 1648-1658; b) Y. Fu, T. Huang, L. Zhang, J. Zhu, X. Wang, *Nanoscale* **2015**, *7*, 13723-13733; c) F. Chen, H. Yang, W. Luo, P. Wang, H. Yu, *Chinese J. Catal.* **2017**, *38*, 1990-1998.

[16] a) J. A. Singh, S. H. Overbury, N. J. Dudney, M. Li, G. M. Veith, *ACS Catal.s* **2012**, *2*, 1138-1146; b) L. Qu, N. Wang, H. Xu, W. Wang, Y. Liu, L. Kuo, T. P. Yadav, J. Wu, J. Joyner, Y. Song, H. Li, J. Lou, R. Vajtai, P. M. Ajayan, *Adv. Func. Mater.* **2017**, *27*, 1701714; c) W. Cheng, H. Su, F. Tang, W. Che, Y. Huang, X. Zheng, T. Yao, J. Liu, F. Hu, Y. Jiang, Q. Liu, S. Wei, *J. Mater. Chem. A* **2017**, *5*, 19649-19655; d) K. Leng, W. Mai, X. Zhang, R. Liu, X. Lin, J. Huang, H. Lou, Y. Xie, R. Fu, D. Wu, *Chem. Commun.* **2018**, *54*, 7159-7162.

[17] H. Li, Y. Xu, H. Sitinamaluwa, K. Wasalathilake, D. Galpaya, C. Yan, *Chinese J. Catal.* **2017**, *38*, 1006-1010.

[18] a) L. Xiao, Y. Jun, B. Wu, D. Liu, T. T. Chuong, J. Fan, G. D. Stucky, *J. Mater. Chem. A* **2017**, *5*, 6382-6387; b) T. Ye, D. P. Durkin, N. A. Banek, M. J. Wagner, D. Shuai, *ACS Appl. Mater. Interfaces* **2017**, *9*, 27421-27426; c) L. Bi, X. Gao, Z. Ma, L. Zhang, D. Wang, T. Xie, *ChemCatChem* **2017**, *9*, 3779-3785; d) W. Wang, Z. Lu, Y. Luo, A. Zou, Q. Yao, X. Chen, *ChemCatChem* **2018**, *10*, 1620-1626.

[19] Y. Cheng, S. Zhao, B. Johannessen, J. Veder, M. Saunders, M. R. Rowles, M. Cheng, C. Liu, M. F. Chisholm, R. De Marco, H. Cheng, S. Yang, S. P. Jiang, *Adv. Mater.* **2018**, *30*, 1706287

[20] a) S. Y. Ding, J. Gao, Q. Wang, Y. Zhang, W. Song, C. Su, W. Wang, *J. Am. Chem. Soc.* **2011**, *133*, 19816-19822; b) M. Shakeri, C. Tai, E. Göthelid, S. Oscarsson, J. Bäckvall, *Chem. Eur. J.* **2011**, *17*, 13269-13273; c) C. M. A. Parlett, P. Keshwalla, S. G. Wainwright, D. W. Bruce, N. S. Hondow, K. Wilson, A. F. Lee, *ACS Catal.* **2013**, *3,* 2122-2129; d) L. Li, H. Zhao, J. Wang, R. Wang, *ACS Nano* **2014**, *8*, 5352-5364; e) H. Zhong, C. Liu, Y. Wang, R. Wang, M. Hong, *Chem. Sci.* **2016**, *7*, 2188-2194; f) S. K. Surmiak, C. Doerenkamp, P. Selter, M. Peterlechner, A. H. Schäfer, H. Eckert, A. Studer, *Chem. Eur. J.* **2017**, *23*, 6019-6028; g) Y. Landais, S. Pramanik, V. Liautard, A. Fernandes, F. Robert, M. Pucheault, *Chem. Eur. J.* **2018**, DOI: 10.1002/chem.201803989.

[21] a) C. Z. Wu, M. Kraume, M. B. Ansorge-Schumacher, *ChemCatChem* **2011**, *3*, 1314-1319; b) K. Gawlitza, C. Z. Wu, R. Georgieva, D. Y. Wang, M. B. Ansorge-Schumacher, R. von Klitzing, *Phys. Chem. Chem. Phys.* **2012**, *14*, 9594-9600.

[22] a) O. Verho, J. E. Bäckvall, *J. Am. Chem. Soc.* **2015**, *137*, 3996-4009; b) C. Palo-Nieto, S. Afewerki, M. Anderson, C.-W. Tai, P. Berglund, A. Córdova, *ACS Catal.* **2016**, *6*, 3932-3940.

[23] a) R. A. Sheldon, *Org. Process Res. Dev.* **2011**, *15*, 213-223; b) R. A. Sheldon, S. van Pelt, *Chem. Soc. Rev.* **2013**, *42*, 6223-6235; c) S. Talekar, A. Joshi, G. Joshi, P. Kamat, R. Haripurkar, S. Kambale, *RSC Adv.* **2013**, *3*, 12485-12511; d) R. A. Sheldon, *Appl. Microbiol. Biot.* **2011**, *92*, 467-477; e) W. Zhang, H. Yang, W. Liu, N. Wang, X. Yu, *Molecules* **2017**, *22,* 2157; f) J. Lee, J. Kim, J. Kim, H. Jia, M. I. Kim, J. H. Kwak, S. Jin, A. Dohnalkova, H. G. Park, H. N. Chang, P. Wang, J. W. Grate, T. Hyeon, *Small* **2005**, *1*, 744-753.

[24] M. Marciello, M. Filice, J. M. Palomo, *Catal. Sci. Technol.* **2012**, *2*, 1531-1543.

[25] J. Xu, M. Antonietti, *J. Am. Chem. Soc.***2017**, *139*, 6026-6029.

[26] a) Y. Wu, M. Wen, M. Navlani-Garcia, Y. Kuwahara, K. Mori, H. Yamashita, *Chem. Asian J.* **2017**, *12*, 860-867; b) B. Sun, H. Yu, Y. Yang, H. Li, C. Zhai, D. Qian, M. Chen, *Phys. Chem. Chem. Phys.* **2017**, *19*, 26072-26084.

[27] H. Wang, W. Zhou, P. Li, X. Tan, Y. Liu, W. Hu, J. Ye, T. Yu, *J. Phys. Chem. C* **2018,** *122*, 17261-17267.

[28] H. Park, J. H. Lee, E. H. Kim, K. Y. Kim, Y. H. Choi, D. H. Youn, J. S. Lee, *Chem. Commun.* **2016**, *52*, 14302-14305.

[29] L. Li, H. Zhao, J. Wang, R. Wang, *ACS Nano* **2014**, *8*, 5352-5364.

[30] E. Vorobyeva, Z. Chen, S. Mitchell, R. K. Leary, P. Midgley, J. M. Thomas, R. Hauert, E. Fako, N. López, J. Pérez-Ramírez, *J. Mater. Chem. A* **2017**, *5*, 16393-16403.

[31] a) A. Saadi, Z. Rassoul, M. M. Bettahar, *J. Mol. Catal. A: Chem.* **2006**, *258*, 59-67; b) M. Castano, K. S. Seo, K. Guo, M. L. Becker, C. Wesdemiotis, J. E. Puskas, *Polym. Chem.* **2015**, *6*, 1137-1142.

[32] M. M. Bradford, *Anal. Biochem.* **1976**, *72*, 248-254.

[33] D. R. Radu, C. Y. Lai, K. Jeftinija, E. W. Rowe, S. Jeftinija, V. S. Lin, *J. Am. Chem. Soc.* **2004**, *126*, 13216-13217.

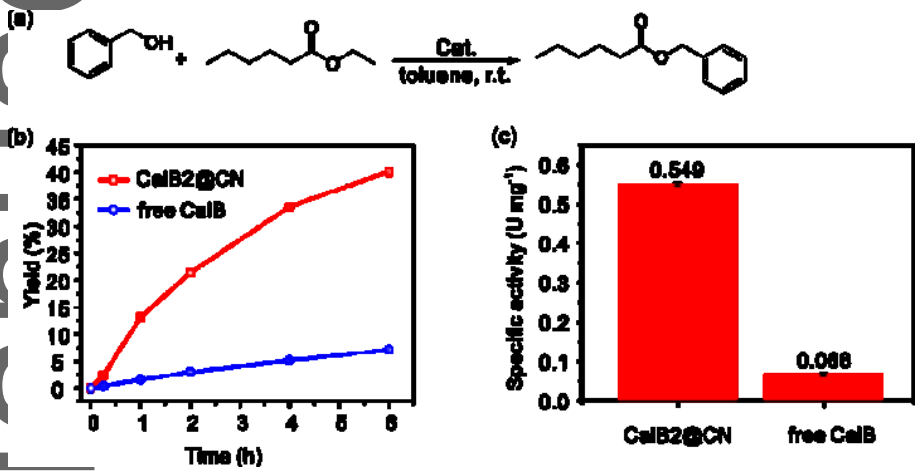

Figure 1. (a) Transesterification catalysed by CalB2@CN; (b) yield of benzyl hexanoate against time catalysed by CalB2@CN and free CalB; (c) specific activity CalB2@CN and free CalB. Reaction conditions: benzyl alcohol (400 mM), ethyl hexanoate (800 mM), CalB2@CN (20 mg) or free CalB (4 mg), toluene (250 µL), 25 °C. One unit of CalB (U) is defined as 1 µmol benzyl hexanoate produced per min, and the specific activity is related to the normalized amount of CalB (U mg^{-1}).

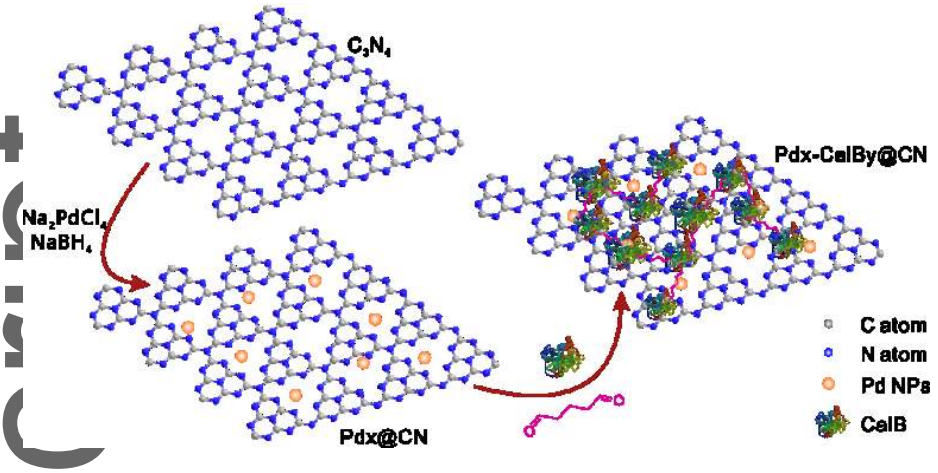

Scheme 1. Schematic illustration of the preparation of biohybrid catalysts. The number x and y mean that the weight percentage of Pd and CalB to C_3N_4 in biohybrid catalysts is x% and y%, respectively.

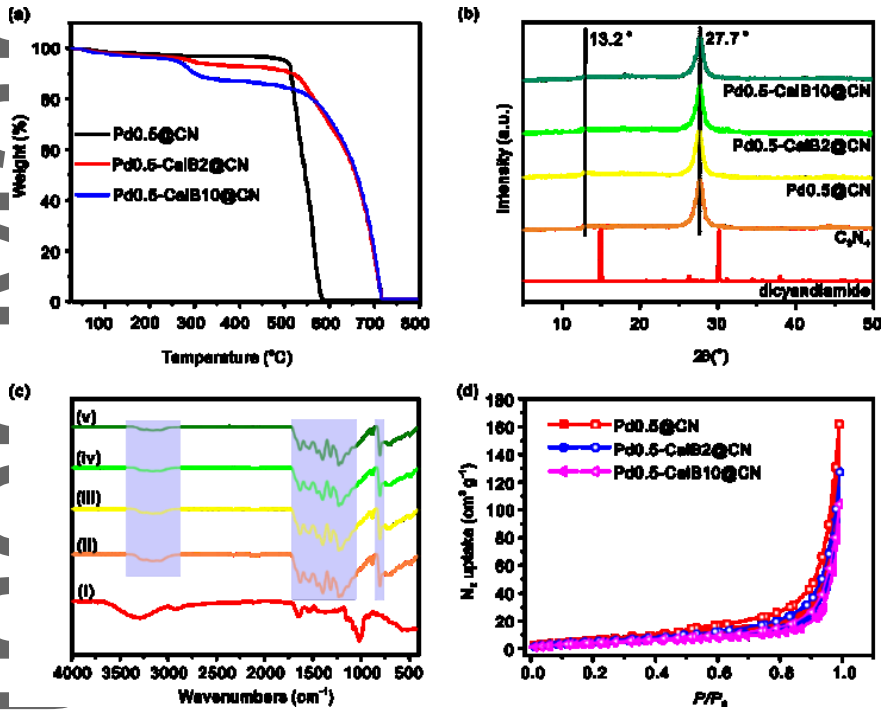

Figure 2. (a) TGA curves of Pd0.5@CN, Pd0.5-CalB2@CN, and Pd0.5-CalB10@CN; (b) PXRD patterns of carbon nitride, Pd0.5@CN, Pd0.5-CalB2@CN, and Pd0.5-CalB10@CN; (c) FTIR spectra of (i) CalB, (ii) C_3N_4, (iii) Pd0.5@CN, (iv) Pd0.5-CalB2@CN, and (v) Pd0.5-CalB10@CN; (d) Nitrogen adsorption/desorption isotherms of Pd0.5@CN, Pd0.5-CalB2@CN, and Pd0.5-CalB10@CN measured at 77 K.

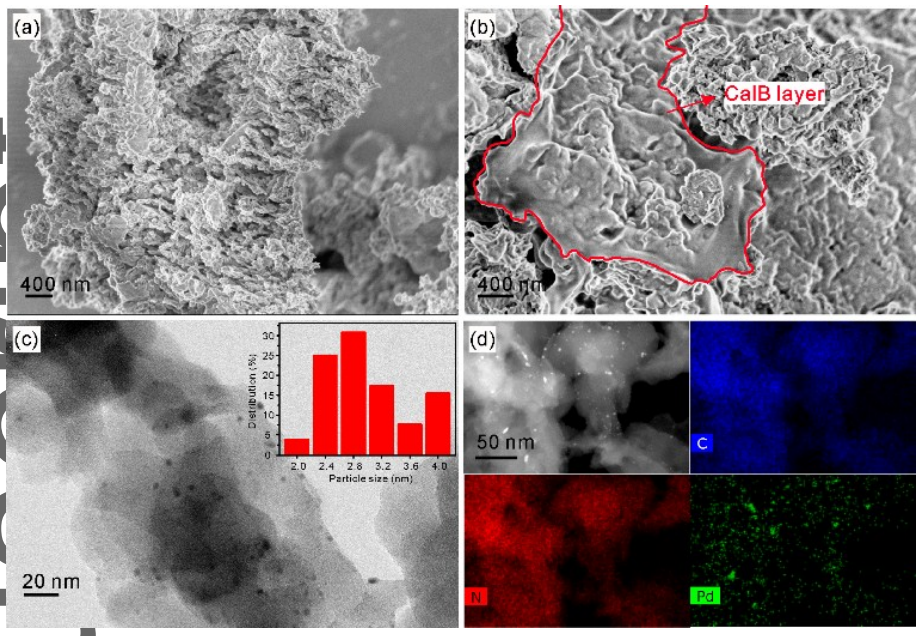

Figure 3. (a) SEM image of C_3N_4; (b) SEM image of Pd0.5-CalB2@CN; (c) bright-field TEM image of Pd0.5-CalB2@CN (insert: Pd particle size distribution); (d) HAADF-STEM micrograph and corresponding carbon, nitrogen and palladium element distributions for Pd0.5-CalB2@CN.

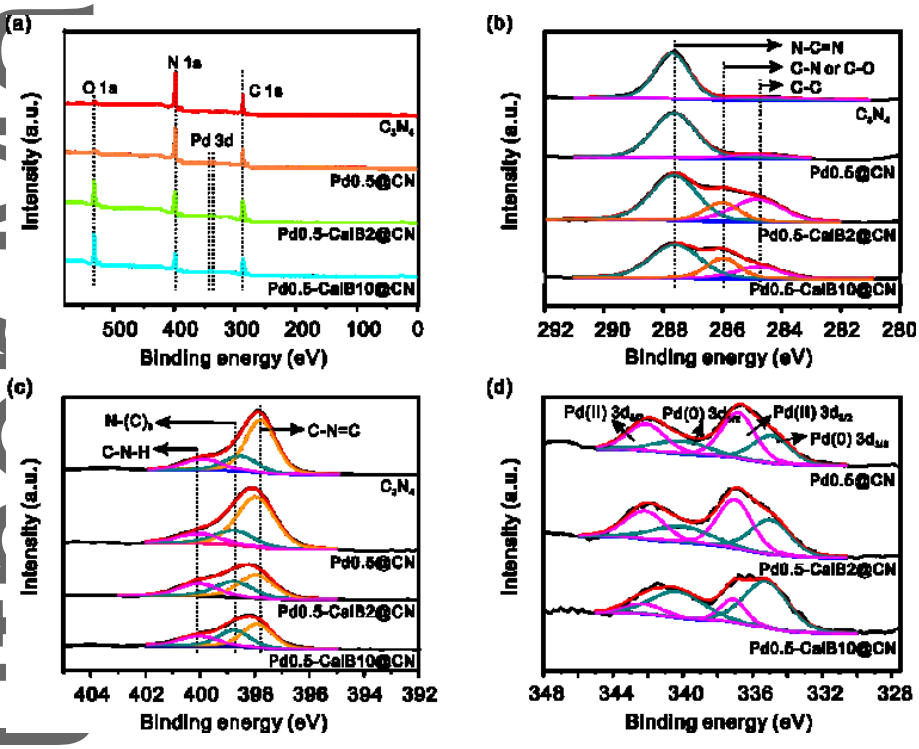

Figure 4. (a) XPS survey spectra and core level spectra of C 1s (b), N 1s (c), and Pd 3d (d) for C_3N_4, Pd0.5@CN, Pd0.5-CalB2@CN, and Pd0.5-CalB10@CN.

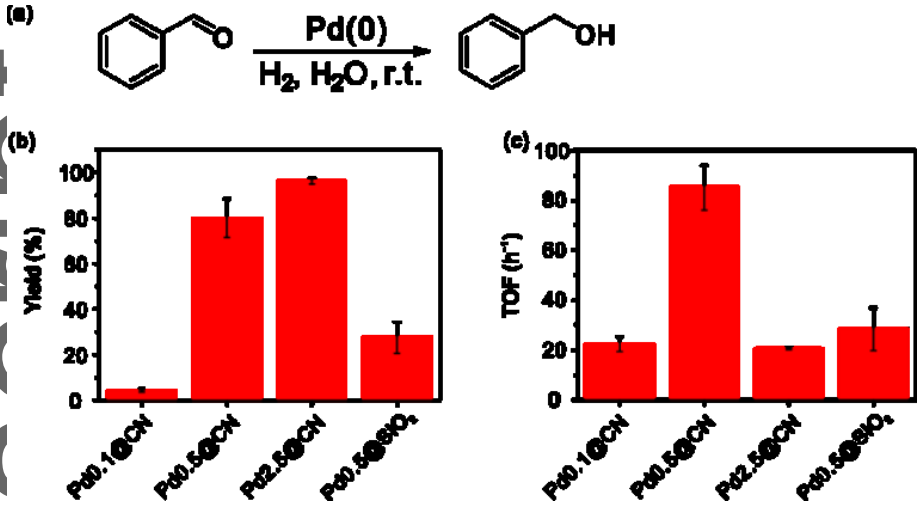

Figure 5. (a) Hydrogenation of benzaldehyde to benzyl alcohol; (b) Yield of benzyl alcohol when using catalyst containing different amount of Pd; (c) TOF of benzaldehyde hydrogenation using catalysts containing different amount of Pd.

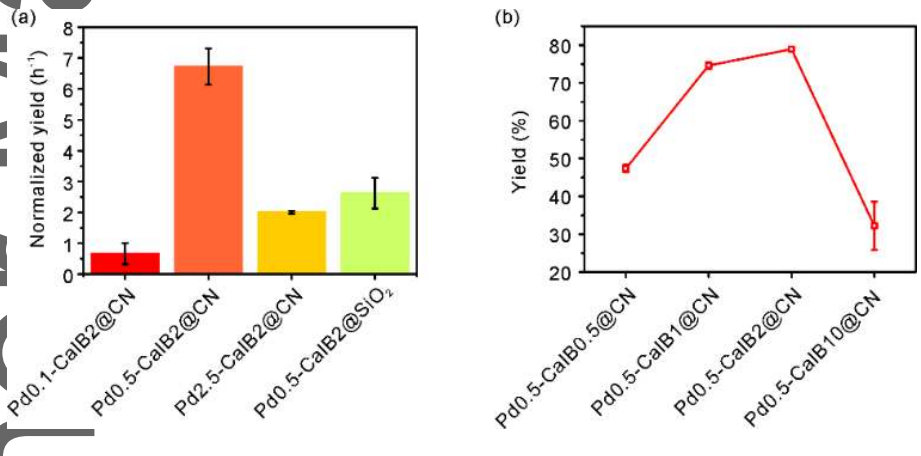

Figure 6. (a) Normalized yield of benzyl hexanoate when using different catalysts containing different amount of Pd but the same amount of CalB; (b) Yield of benzyl hexanoate when using different catalysts containing the same amount of Pd but different amount of CalB.

The exploration of new platforms for fabricating highly efficient and durable biohybrid catalysts for cascade reactions is an attractive subject of practical interest. In this work, carbon nitride (C_3N_4) is utilized as solid support for the first time to co-immobilize Pd nanoparticles and *Candida antarctica* lipase B for preparing biohybrid catalysts. The as-synthesized catalysts show high catalytic efficiency in a cascade reacton converting benzaldyde to benzyl hexanoate.

Keyword cascade reaction

Y. Wang, N. Zhang, R. Hübner, D. Tan, M. Löffler, S. Facsko, E. Zhang, Y. Ge,* Z. Qi,* and C. Wu*

Enzymes immobilized on carbon nitride (C_3N_4) cooperating with metal nanoparticles for cascade catalysis